essentially induced by local modifications of the electronic properties of a surface near chemisorbed particles and hence, we believe, are of general importance for chemical processes at surfaces whenever the diffusion lengths of adsorbing species reach critical values compared with their lateral distribution. □

1. Boudart, M. & Djega-Mariadassow, G. *Kinetics of Heterogeneous Catalytic Reactions* (Princeton Univ. Press, 1984).
2. Gland, J. L. Molecular and atomic adsorption of oxygen on the Pt(111) and Pt(S)-12(111) × (111) surfaces. *Surf. Sci.* **93**, 487–514 (1980).
3. Gland, J. L., Sexton, B. A. & Fisher, G. B. Oxygen interaction with the Pt(111) surface. *Surf. Sci.* **95**, 587–602 (1980).
4. Campbell, C. T., Ertl, G., Kuipers, H. & Segner, J. A molecular beam study of the adsorption and desorption of oxygen from a Pt(111) surface. *Surf. Sci.* **107**, 220–236 (1981).
5. Steininger, H., Lehwald, S. & Ibach, H. Adsorption of oxygen on Pt(111). *Surf. Sci.* **123**, 1–17 (1982).
6. Avery, N. R. An EELS and TDS study of molecular oxygen desorption and decomposition on Pt(111). *Chem. Phys. Lett.* **96**, 371–373 (1983).
7. Luntz, A. C., Williams, M. D. & Bethune, D. S. The sticking of O_2 on a Pt(111) surface. *J. Chem. Phys.* **89**, 4381–4395 (1988).
8. Williams, M. D., Bethune, D. S. & Luntz, A. C. Coexistence of precursor and direct dynamics: The sticking of O_2 on a Pt(111) surface. *J. Chem. Phys.* **88**, 2843–2845 (1988).
9. Winkler, A., Guo, X., Siddiqui, H. R., Hagans, P. L. & Yates, J. J. T. Kinetics and energetics of oxygen adsorption on Pt(111) and Pt(112)—a comparison of flat and stepped surfaces. *Surf. Sci.* **201**, 419–443 (1988).
10. Luntz, A. C., Grimblot, J. & Fowler, D. E. Sequential precursors in dissociative chemisorption: O_2 on Pt(111). *Phys. Rev. B* **39**, 12903–12906 (1989).
11. Wurth, W. *et al.* Bonding, structure, and magnetism of physisorbed and chemisorbed O_2 on Pt(111). *Phys. Rev. Lett.* **65**, 2426–2429 (1990).
12. Rettner, C. T. & Mullins, C. B. Dynamics of the chemisorption of O_2 on Pt(111): Dissociation via direct population of a molecularly chemisorbed precursor at high incidence kinetic energy. *J. Chem. Phys.* **94**, 1626–1635 (1991).
13. Puglia, C. *et al.* Physisorbed, chemisorbed and dissociated O_2 on Pt(111) studied with different core level spectroscopy methods. *Surf. Sci.* **342**, 119–133 (1995).
14. Wintterlin, J., Schuster, R. & Ertl, G. Existence of a "hot" atom mechanism for the dissociation of O_2 on Pt(111). *Phys. Rev. Lett.* **77**, 123–126 (1996).
15. Artsykhovich, A. N., Ukraintsev, V. A. & Harrison, I. Low temperature sticking and desorption dynamics of oxygen on Pt(111). *Surf. Sci.* **347**, 303–318 (1996).
16. Stipe, B. C. *et al.* Single-molecule dissociation by tunneling electrons. *Phys. Rev. Lett.* **78**, 4410–4413 (1997).
17. Witten, T. A. & Sander, L. M. Diffusion-limited aggregation, a kinetic critical phenomenon. *Phys. Rev. Lett.* **47**, 1400–1403 (1981).

Effect of seawater carbonate concentration on foraminiferal carbon and oxygen isotopes

Howard J. Spero*, **Jelle Bijma**†, **David W. Lea**‡
& Bryan E. Bemis*

* *Department of Geology, University of California Davis, Davis, California 95616, USA*
† *Alfred Wegener Institute for Polar and Marine Research, PO Box 120161, D-27515 Bremerhaven, Germany*
‡ *Department of Geological Sciences and the Marine Science Institute, University of California Santa Barbara, Santa Barbara, California 93106, USA*

....

Stable oxygen and carbon isotope measurements on biogenic calcite and aragonite have become standard tools for reconstructing past oceanographic and climatic change. In aquatic organisms, $^{18}O/^{16}O$ ratios in the shell carbonate are a function of the ratio in the sea water and the calcification temperature[1]. In contrast, $^{13}C/^{12}C$ ratios are controlled by the ratio of dissolved inorganic carbon in sea water and physiological processes such as respiration and symbiont photosynthesis[2]. These geochemical proxies have been used with analyses of foraminifera shells to reconstruct global ice volumes[3], surface and deep ocean temperatures[4,5], ocean circulation changes[6] and glacial–interglacial exchange between the terrestrial and oceanic carbon pools[7]. Here, we report experimental measurements on living symbiotic and non-symbiotic plankton foraminifera (*Orbulina universa* and *Globigerina bulloides* respectively) showing that the $^{13}C/^{12}C$ and $^{18}O/^{16}O$ ratios of the calcite shells decrease with increasing seawater $[CO_3^{2-}]$. Because glacial-period oceans had higher pH and $[CO_3^{2-}]$ than today[8], these new relationships confound the standard interpretation of glacial foraminiferal stable-isotope data. In particular, the hypothesis that the glacial–interglacial shift in the $^{13}C/^{12}C$ ratio was due to a transfer of terrestrial carbon into the ocean[7] can be explained alternatively by an increase in ocean alkalinity[25]. A carbonate-concentration effect could also help explain some of the extreme stable-isotope variations during the Proterozoic and Phanerozoic aeons[9].

Data from isotopic calibration studies suggest that a previously unidentified parameter affects carbon and oxygen isotope ratios in foraminiferal shells[10]. Generally, observations of disequilibrium precipitation have been attributed to respiration or symbiont photosynthesis. These physiological processes contribute ^{13}C-depleted CO_2 to the calcifying microenvironment (respiration) or enrich the environment in ^{13}C via preferential removal of $^{12}CO_2$ (photosynthesis)[2]. In contrast, shell $^{18}O/^{16}O$ ratios should be insensitive to physiology. Yet data demonstrate[11] that shell $\delta^{18}O$ is often out of equilibrium with respect to temperature and $\delta^{18}O_{water}$ (see Methods). Laboratory and field data show that the $\delta^{18}O$ and $\delta^{13}C$ of $CaCO_3$ can covary[11,12], suggesting that a common mechanism affects the isotope ratios of both elements.

Our experimental results demonstrate that at constant alkalinity, but varying ΣCO_2, the $\delta^{13}C$ and $\delta^{18}O$ of *O. universa* shells decrease by about 3.9‰ and 1.5‰ respectively as $[CO_3^{2-}]$ increases from 100 to 642 $\mu mol\,kg^{-1}$ (see Methods and Fig. 1a, b). Shell $\delta^{13}C$ and $\delta^{18}O$ values remain constant when seawater $[CO_3^{2-}]$ is further reduced from 100 to 41 $\mu mol\,kg^{-1}$. Comparison of foraminifera grown under photosynthetic maximum (P_{max}) light levels[13] (denoted HL) with specimens maintained in the dark (D) (to compare maximum with minimum symbiont photosynthetic activity), shows that P_{max} shells are consistently enriched in ^{13}C by 1.1‰ and depleted in ^{18}O by 0.3‰ relative to dark specimens. Although this effect has been documented previously[14], the constant offset, and the identical regression slopes (-0.0063 ± 0.0007 (HL) (95% confidence interval) and -0.0061 ± 0.0013‰/($\mu mol\,kg^{-1}$) (D) for $\delta^{13}C/[CO_3^{2-}]$, and -0.0022 ± 0.0006 (HL) and -0.0019 ± 0.0002‰/($\mu mol\,kg^{-1}$) (D) for $\delta^{18}O/[CO_3^{2-}]$) demonstrate that symbiont photosynthesis is not responsible for the observed relationships between isotopes and $[CO_3^{2-}]$.

In a second experiment, we manipulated $[CO_3^{2-}]$ between 75 and 774 $\mu mol\,kg^{-1}$ by varying alkalinity and maintaining ΣCO_2 at $2,032 \pm 15\,\mu mol\,kg^{-1}$ (Fig. 1c and d). Again, $\delta^{13}C$ and $\delta^{18}O$ in *O. universa* shells decreased as $[CO_3^{2-}]$ increased, with regression slopes of -0.0055 ± 0.0015 (HL) and -0.0060 ± 0.0015‰/($\mu mol\,kg^{-1}$) (D) for carbon and -0.0015 ± 0.0008 (HL) and -0.0022 ± 0.0004‰/($\mu mol\,kg^{-1}$) (D) for oxygen. For a companion experiment, several *O. universa* were removed from sea water of high $[CO_3^{2-}]$ (458 $\mu mol\,kg^{-1}$) after sphere formation but before gametogenesis to test whether the carbonate ion effect was due to inorganic precipitation on the surface of empty, post-gametogenic shells. The $\delta^{13}C$ and $\delta^{18}O$ values of both pre- and post-gametogenic shells were identical, indicating that the relationship is a function of calcification during normal shell growth. Furthermore, because the seawater carbonate chemistry in our experiments was modified two ways yet produced indistinguishable regression slopes, the relationship between isotopic ratios and $[CO_3^{2-}]$ is real and not an artefact of our experiments.

In a final experiment, we cultured a nonsymbiotic species, *G. bulloides*, across a $[CO_3^{2-}]$ range of 103–436 $\mu mol\,kg^{-1}$ at constant ΣCO_2. Because *G. bulloides* displays a large chamber-to-chamber ontogenetic effect for both $\delta^{13}C$ and $\delta^{18}O$[11], we amputated those chambers secreted during the experiments and pooled chambers from discrete positions in the shell whorl for isotope measurement

(Fig. 2). Regression analysis of data from the 12th and 13th chambers yields slopes of −0.012 to −0.014 for $\delta^{13}C/[CO_3^{2-}]$ and −0.004 to −0.005 for $\delta^{18}O/[CO_3^{2-}]$, demonstrating that ontogeny has little affect on this relationship. Interestingly, the *G. bulloides* regression slopes are twice those of *O. universa*, suggesting that the slope of the carbonate ion effect is species-specific.

We recognize that these experiments extend beyond the present seawater $[CO_3^{2-}]$ range as well as that proposed for the last glacial maximum[8]. Statistical analysis of data from the constant-alkalinity experiment on *O. universa*, which encompasses the proposed Quaternary $[CO_3^{2-}]$ range (100–400 μmol kg^{-1}), yields slopes that are indistinguishable (within 95% confidence intervals) from the full data sets with exception of the dark $\delta^{13}C/[CO_3^{2-}]$ slope of −0.0033‰/(μmol kg^{-1}). Because we have higher confidence in the stable isotope/$[CO_3^{2-}]$ slopes calculated from the entire experimental range, we use those values for discussion in the following sections.

Evidence for a similar isotope effect exists in corals and other invertebrate groups that display a $\delta^{18}O:\delta^{13}C$ covariance[15]. For instance, in the nonphotosynthetic coral, *Tubastrea*, isotope values covary with a positive $\delta^{18}O/\delta^{13}C$ slope of 0.29. The foraminiferal $\delta^{18}O/\delta^{13}C$ relationships obtained here are virtually identical, with slopes ranging between 0.29 and 0.33 (Fig. 3). Other ahermatypic corals, calcareous algae and invertebrates such as cidaroid urchins show oxygen and carbon isotope covariance[15,16], although the slopes can differ from the experimental range. In symbiont-bearing organisms such as the coral *Pavona* or foraminifer *Globigerinoides sacculifer*, the slope can change sign because of the additional ^{13}C-enriching effect of symbiont photosynthesis[15,17]. Aside from organisms that display a large symbiont effect, the similarities in the slope of the relationship among different protozoans, invertebrates and calcifying algae suggests that related mechanisms are responsible for the isotope covariance.

Comparison of our experimental data with results for inorganic precipitates[18] shows remarkable similarity in $\delta^{18}O$ variations with $[CO_3^{2-}]$ (Fig. 4). McCrea demonstrated that the $^{18}O/^{16}O$ ratio of rapidly precipitated $CaCO_3$ decreases with increasing percentage of CO_3^{2-} in solution and suggested that the calcification rate plays a role. The similarity between biological and inorganic precipitate studies implicates a kinetic mechanism which may affect all calcifying organisms and inorganic precipitates. Although we cannot estimate the calcification rates of *O. universa* in our experiments, shell mass measurements on high light and dark groups show that specimens grown in high $[CO_3^{2-}]$ (over 600 μmol kg^{-1}) are 37% heavier than those in ambient sea water. Because the *O. universa* lifespan was similar for the different treatments, heavier shells probably indicate higher calcification rates. Chamber mass data for *G. bulloides* are inconclusive.

Although we cannot offer a definitive mechanism for the isotope:$[CO_3^{2-}]$ relationships, mass balance calculations show that the results cannot be explained by a simple redistribution of isotopes between the dissolved carbon species[19]. MConnaughey[12]
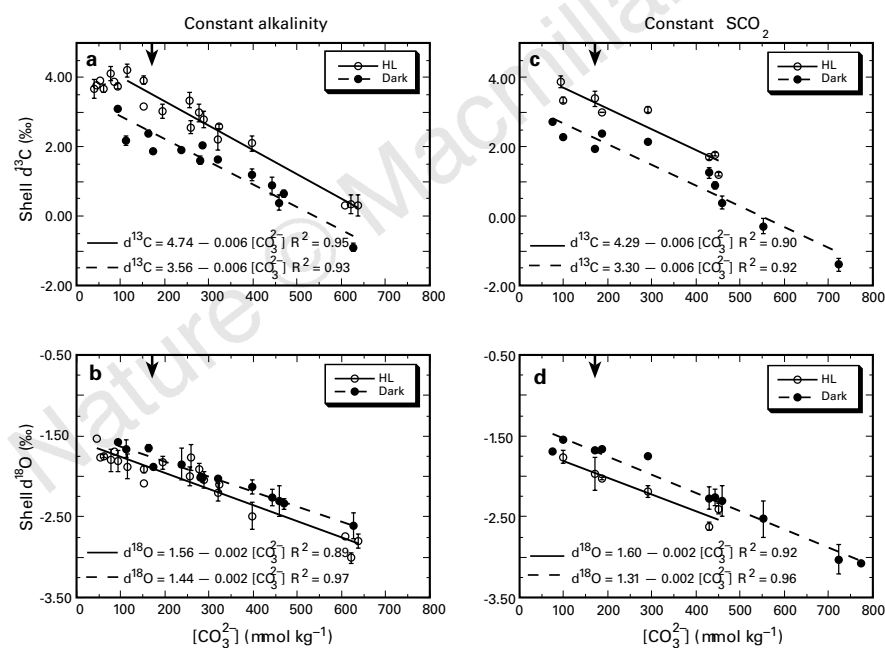
Figure 1 Effect of $[CO_3^{2-}]$ on the $\delta^{13}C$ and $\delta^{18}O$ values of *Orbulina universa* shell calcite under conditions of constant alkalinity (**a** and **b**) and constant ΣCO_2 (**c** and **d**) conditions. Specimens grown under high light and in the dark are shown by open and closed circles respectively. Arrowheads identify ambient $[CO_3^{2-}]$ in the Southern California Bight. Data are group mean values ±1 s.d.; most groups are composed of 3–10 individual shells. Lines are linear regressions fitted to the data.
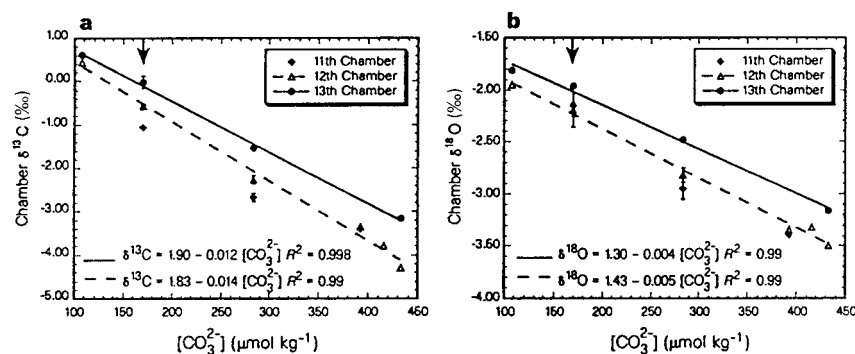
Figure 2 Effect of $[CO_3^{2-}]$ on the $\delta^{13}C$ and $\delta^{18}O$ values of *Globigerina bulloides* chamber calcite under constant ΣCO_2 conditions. Data are from pooled, amputated chambers from specific positions in the shell whorl. Linear regression analyses are plotted for data from chambers 12 and 13, the last two chambers in the shell.
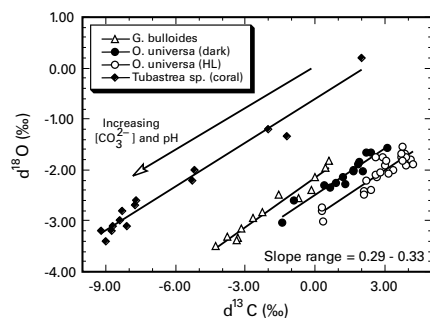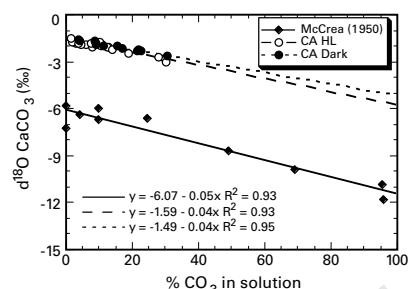
Figure 3 Comparison of foraminiferal $\delta^{13}C$ and $\delta^{18}O$ data from all experiments with data from the nonsymbiotic coral, *Tubastrea* spp. (ref. 15). The similarity of the positive covariance between coral (aragonite) and foraminifera (calcite) stable isotopes suggests that a similar mechanism is responsible for the observed variations. In this plot, $[CO_3^{2-}]$ and pH increase towards the origin.

Figure 4 Comparison of high light and dark *O. universa* $\delta^{18}O$ data from the constant alkalinity (CA) experiment with inorganic precipitate results from McCrea[18]. Oxygen isotope data are plotted against % CO_3^{2-} in solution, where % $CO_3^{2-} = [CO_3^{2-}]/([CO_3^{2-}] + [HCO_3^-]) \times 100$. Note that the slopes of our experimental data are indistinguishable from that obtained by McCrea.

has explained the strong $\delta^{13}C:\delta^{18}O$ covariance in the coral *Tubastrea* by a combination of 'kinetic' and 'metabolic' isotope effects. The kinetic effect is attributed to slower CO_2 hydration and hydroxylation reactions by molecules enriched in the heavier isotopes ^{13}C and ^{18}O. McConnaughey further argues that CO_2 hydration and hydroxylation reactions may show different kinetic isotope effects and that the balance between these two reactions changes with pH. At high pH and $[CO_3^{2-}]$, CO_3^{2-} favours the lighter isotope in the exchange of oxygen atoms between CO_2 and CO_3^{2-}. A similar mechanism was proposed by McCrea[18] and has been supported by more recent work[20].

In contrast, metabolic effects can be attributed to the incorporation of ^{13}C-depleted respired CO_2. For aquatic organisms, such respiratory effects may be small and difficult to evaluate against the larger kinetic effect[21]. In some benthic foraminifera, an internal inorganic carbon pool can introduce added complexity when one attempts to resolve the carbon sources controlling shell $\delta^{13}C$[22]. Although a carbon pool is absent in *O. universa* (J.B., unpublished data), metabolic carbon does contribute 8–15% to *G. bulloides* shell carbon[11]. Such differences in carbon sources might explain the species-specific $\delta^{13}C/[CO_3^{2-}]$ slopes observed here but would not be expected to influence $\delta^{18}O$. Current experiments should help to constrain the active mechanism(s).

Because the CO_2 partial pressure (p_{CO_2}) of the sea surface and the atmosphere must be in approximate equilibrium, the glacial drop in atmospheric carbon dioxide recorded in ice cores[23,24] must have been accompanied by an increase in surface water $[CO_3^{2-}]$. Therefore shells calcifying during cold periods record isotopic signatures that cannot be interpreted using present-day relationships. Our calculations indicate that to achieve equilibrium with a glacial atmospheric p_{CO_2} of 200 parts per million by volume (p.p.m.V), surface water $[CO_3^{2-}]$ must have increased by a minimum of 40 μmol kg^{-1}, with considerably larger changes possible depending on sea surface temperature (SST) and the actual mode of p_{CO_2} change[25]. Combining this conservative estimate with the experimental relationships presented here suggests that the glacial rise in $[CO_3^{2-}]$ can account for at least a 0.25–0.5‰ drop in shell $\delta^{13}C$, with the larger change characterizing *G. bulloides*. Large glacial-to-interglacial (G–I) shifts, 0.7‰ or greater, observed in $\delta^{13}C$ records from *G. bulloides*[26] are consistent with the greater response of this species to $[CO_3^{2-}]$. The smaller glacial shifts recorded in tropical records of *G. sacculifer* (0.3‰)[27] suggest a $[CO_3^{2-}]$ response for this species that is similar to *O. universa*, a hypothesis that can be tested experimentally. If some or all of the negative carbon isotope shift that is common to all species can be attributed to an increase in $[CO_3^{2-}]$, this reduces the actual G–I mean shift in $\delta^{13}C$ for the ocean. This would enlarge the difference between pollen-based and ocean-$\delta^{13}C$-based estimates of the amount of carbon transferred from the terrestrial biosphere to

the ocean during glacial episodes[7,28].

The influence of $[CO_3^{2-}]$ also confounds the interpretation of $\delta^{13}C$ differences between planktic and benthic foraminifera as a measure of the efficiency of the biological pump[26]. Because a 0.1‰ increase in $\Delta\delta^{13}C$ translates to an approximate 10 p.p.m.V drop in p_{CO_2}, a 0.3‰ correction on planktics, which is the minimum calculated, can explain an additional glacial-interglacial p_{CO_2} difference of 30 p.p.m.V, implying a stronger glacial biological pump than previously indicated[27]. However, this calculation depends on the magnitude of the $[CO_3^{2-}]$ influence on planktic species for which experimental data are not available, and it must also take into account a potential $[CO_3^{2-}]$ influence on benthic shell $\delta^{13}C$ which has not yet been demonstrated. Correcting for the more subtle influence of $[CO_3^{2-}]$ on shell $\delta^{18}O$ lowers glacial tropical SST estimates by up to 1 °C, bringing oxygen isotope palaeotemperatures closer to those calculated from other marine SST proxies (such as coral Sr/Ca ratios) and terrestrial indicators (such as snowline and ice-core $\delta^{18}O$) that suggest more intense tropical cooling at the last glacial maximum[29,30].

The late Proterozoic and early Phanerozoic aeons must have had very different ocean carbonate chemistries from the present in order to maintain high p_{CO_2} and accumulate extensive carbonate platforms[31,32]. Higher ΣCO_2, alkalinity and/or $[CO_3^{2-}]$ could satisfy both requirements. If a carbonate ion effect were operating, higher $[CO_3^{2-}]$ would result in $CaCO_3$ with lower $\delta^{13}C$ and $\delta^{18}O$ values than predicted from current ocean chemistry. Large negative $\delta^{13}C$ excursions have been recorded throughout the late Proterozoic, especially near the Vendian/Cambrian boundary[9]. In the early Palaeozoic, very low $\delta^{13}C$ and $\delta^{18}O$ values have been recovered from articulate brachiopods[33]. Could changes in ocean carbonate chemistry help to explain some of these observations? □

Methods

Collection and culturing. *O. universa* and *G. bulloides* were collected by scuba divers from surface waters of the San Pedro Basin, Southern California Bight, USA, and were maintained in laboratory culture at 22 ± 0.2 °C at the Wrigley Institute of Environmental Science on Santa Catalina Island. Specimens were grown in 0.8-μm-filtered sea water in sealed, air-tight 125 mL acid-cleaned Pyrex jars and fed a one-day-old *Artemia* nauplius every third day (total time in culture ~6–8 days). For *O. universa*, specimens were maintained either in the dark or under P_{max} light levels (400–700 μEinst $m^{-2} s^{-1}$; 1 einstein = 1 mole photons)[13] to quantify the effect of symbiont photosynthesis on the relationship between stable isotopes and $[CO_3^{2-}]$. Following gametogenesis, the empty foraminiferal shells were archived for analysis. *G. bulloides* chambers secreted during the experiments were amputated from the shell whorl and pooled according to chamber position[11]. In *O. universa*, a single spherical chamber was secreted in the laboratory which accounted for 90–95% of total shell calcite.
Seawater chemistry manipulation. We modified seawater carbonate

chemistry by either: (1) raising total alkalinity (alk_t) (where alkalinity = $[HCO_3^- + 2[CO_3^{2-}] + [HBO_3^-]]$) to constant levels of $2,842 \pm 80 \, \mu eq \, kg^{-1}$ (equivalent = mole of negative or positive charge) ($n = 29$ groups) (ambient $alk_t = 2,241 \pm 19 \, \mu eq \, kg^{-1}$; $n = 64$ groups) and letting ΣCO_2 ($\Sigma CO_2 = [CO_2] + [HCO_3^-] + [CO_3^{2-}]$) and pH vary (pH ranges between 7.38 and 8.83); or (2) keeping ΣCO_2 constant at $2,032 \pm 15 \, \mu mol \, kg^{-1}$ ($n = 15$ groups) (ambient $\Sigma CO_2 = 2,010 \pm 18 \, \mu mol \, kg^{-1}$; $n = 64$ groups) and letting pH and alkalinity vary (pH ranges from 7.87 to 8.97). For comparison with our experiments, pH and $[CO_3^{2-}]$ in Southern California Bight surface waters varied between $8.11–8.19$ and $153–184 \, \mu mol \, kg^{-1}$ during our field campaign.

Seawater ΣCO_2 and alk_t were modified by the addition of Na_2CO_3 and/or titration with HCl or NaOH to bring alk_t to desired levels. Seawater pH was determined by potentiometry whereas alk_t and ΣCO_2 were determined by titration and equilibrium calculations respectively. Coulometric determinations of several seawater samples confirm the accuracy of the calculated ΣCO_2 values (A. Sanyal, personal communication). Culture water samples collected at the start and end of each experiment showed that alkalinity and ΣCO_2 remained constant throughout each experiment.

Stable isotope analyses. Individual *O. universa* shells and *G. bulloides* chambers were roasted at $375 \, °C$ *in vacuo* and analysed with a Fisons Optima isotope ratio mass spectrometer using an Isocarb common acid bath autocarbonate system at $90 \, °C$. Here $\delta^{18}O = [(^{18}O/^{16}O_{sample}/^{18}O/^{16}O_{std}) - 1]$ and $\delta^{13}C = [(^{13}C/^{12}C_{sample}/^{13}C/^{12}C_{std}) - 1]$. All $\delta^{13}C_{\Sigma CO_2}$ and $CaCO_3$ isotope values are relative to the V-PDB standard. Water samples collected at the start and end of each experiment show that $\delta^{18}O_{water}$ was constant at $-0.23 \pm 0.05‰$ (relative to the V-SMOW standard) ($n = 100$) whereas initial and final water $\delta^{13}C_{\Sigma CO_2}$ differed on average by $0.16 \pm 0.10‰$ ($n = 30$). All foraminiferal $\delta^{13}C$ data have been corrected to a constant $\delta^{13}C_{\Sigma CO_2} = 2.00‰$ (ambient $\delta^{13}C_{\Sigma CO_2}$ was $1.90 \pm 0.08‰$, $n = 18$) to account for $\delta^{13}C_{\Sigma CO_2}$ differences between treatments due to the addition of Na_2CO_3.

1. Epstein, S., Buchsbaum, R., Lowenstam, H. A. & Urey, H. C. Revised carbonate-water isotopic temperature scale. *Geol. Soc. Am. Bull.* **64,** 1315–1325 (1953).
2. Spero, H. J., Lerche, I. & Williams, D. F. Opening the carbon isotope "vital effect" black box, 2: Quantitative model for interpreting foraminiferal carbon isotope data. *Paleoceanography* **6,** 639–655 (1991).
3. Shackleton, N. J. & Opdyke, N. D. Oxygen isotope and palaeomagnetic stratigraphy of equatorial Pacific core V28-238: Oxygen isotope temperatures and ice volumes on a 10^5 year and 10^6 year scale. *Quat. Res.* **3,** 39–55 (1973).
4. Broecker, W. S. Oxygen isotope constraints on surface ocean temperatures. *Quat. Res.* **26,** 121–134 (1986).
5. Labeyrie, L. D., Duplessy, J.-C. & Blanc, P. L. Variations in mode of formation and temperature of oceanic deep waters over the past 125,000 years. *Nature* **327,** 477–482 (1987).
6. Duplessy, J. C. *et al.* Deepwater source variations during the last climatic cycle and their impact on the global deepwater circulation. *Paleoceanography* **3,** 343–360 (1988).
7. Shackleton, N. J. Carbon-13 in Uvigerina: tropical rainforest history and the equatorial Pacific carbonate dissolution cycles. in *The Fate of Fossil Fuel CO_2 in the Oceans* (eds Andersen, N. R. & Malahoff, A.) 401–427 (Plenum, New York, 1977).
8. Sanyal, A., Hemming, N. G., Hanson, G. N. & Broecker, W. S. Evidence for a higher pH in the glacial ocean from boron isotopes in foraminifera. *Nature* **373,** 234–236 (1995).
9. Kaufman, A. J., Jacobsen, S. B. & Knoll, A. H. The Vendian record of Sr and C isotopic variations in seawater: Implications for tectonics and paleoclimate. *Earth Planet. Sci. Lett.* **120,** 409–430 (1993).
10. Fairbanks, R. G., Sverdlove, M., Free, R., Wiebe, P. H. & Be, A. W. H. Vertical distribution and isotopic fractionation of living planktonic foraminifera from the Panama Basin. *Nature* **298,** 841–844 (1982).
11. Spero, H. J. & Lea, D. W. Experimental determination of stable isotope variability in *Globigerina bulloides*: Implications for paleoceanographic reconstruction. *Mar. Micropaleontol.* **28,** 231–246 (1996).
12. McConnaughey, T. ^{13}C and ^{18}O isotopic disequilibrium in biological carbonates: II. In vitro simulation of kinetic isotope effects. *Geochim. Cosmochim. Acta* **53,** 163–171 (1989).
13. Spero, H. J. & Parker, S. L. Photosynthesis in the symbiotic planktonic foraminifer *Orbulina universa*, and its potential contribution to oceanic primary productivity. *J. Foram. Res.* **15,** 273–281 (1985).
14. Spero, H. J. Do planktic foraminifera accurately record shifts in the carbon isotopic composition of sea water ΣCO_2? *Mar. Micropaleontol.* **19,** 275–285 (1992).
15. McConnaughey, T. ^{13}C and ^{18}O isotopic disequilibrium in biological carbonates: I. Patterns. *Geochim. Cosmochim. Acta* **53,** 151–162 (1989).
16. Smith, J. E., Risk, M. J., Schwarcz, H. P. & McConnaughey, T. A. Rapid climate change in the North Atlantic during the Younger Dryas recorded by deep-sea corals. *Nature* **386,** 818–820 (1997).
17. Spero, H. J. & Lea, D. W. Intraspecific stable isotope variability in the planktic foraminifera *Globigerinoides sacculifer*: Results from laboratory experiments. *Mar. Micropaleontol.* **22,** 221–234 (1993).
18. McCrea, J. M. On the isotopic chemistry of carbonates and a paleotemperature scale. *J. Chem. Phys.* **18,** 849–857 (1950).
19. Zhang, J., Quay, P. D. & Wilbur, D. O. Carbon isotope fractionation during gas–water exchange and dissolution of CO_2. *Geochim. Cosmochim. Acta* **59,** 107–114 (1995).
20. Usdowski, E. & Hoefs, J. Oxygen isotope exchange between carbonic acid, bicarbonate, carbonate, and water: A re-examination of the data of McCrea (1950) and an expression for the overall partitioning of oxygen isotopes between the carbonate species and water. *Geochim. Cosmochim. Acta* **57,** 3815–3818 (1993).
21. McConnaughey, T. A., Burdett, J., Whelan, J. F. & Paull, C. K. Carbon isotopes in biological carbonates: Respiration and photosynthesis. *Geochim. Cosmochim. Acta* **61,** 611–622 (1997).
22. ter Kuile, B., Erez, J. & Padan, E. Mechanisms for the uptake of inorganic carbon by two species of symbiont-bearing foraminifera. *Mar. Biol.* **103,** 241–251 (1989).
23. Barnola, J. M., Raynaud, D., Korotkevich, Y. S. & Lorius, C. Vostok ice core provides 160,000-year record of atmospheric CO_2. *Nature* **329,** 408–413 (1987).
24. Broecker, W. S. & Peng, T.-H. What caused the glacial to interglacial CO_2 change? in *The Global Carbon Cycle* (ed. Heimann, M.) 95–115 (Springer, Berlin, 1993).
25. Lea, D. W., Spero, H. J., Bijma, J. & Archer, D. Implications of a carbonate ion effect on shell carbon and oxygen isotopes for glacial ocean conditions. *EOS* **77** (46) Fall Meeting Suppl. F334 (1996).
26. Shackleton, N. J., Hall, M. A., Line, J. & Shuxi, C. Carbon isotope data in core V19-30 confirm reduced carbon dioxide concentration in the ice age atmosphere. *Nature* **306,** 319–322 (1983).
27. Shackleton, N. J., Le, J., Mix, A. & Hall, M. A. Carbon isotope records from Pacific surface waters and atmospheric carbon dioxide. *Quat. Sci. Rev.* **11,** 387–400 (1992).
28. Crowley, T. J. Ice age terrestrial carbon changes revisited. *Global Biogeochem. Cycles* **9,** 377–389 (1995).
29. Guilderson, T. P., Fairbanks, R. G. & Rubenstone, J. L. Tropical temperature variations since 20,000 years ago: Modulating interhemispheric climate change. *Science* **263,** 663–665 (1994).
30. Thompson, L. G. *et al.* Late glacial stage and Holocene tropical ice core records from Huascaran, Peru. *Science* **269,** 46–50 (1995).
31. Berner, R. A. Geocarb II: A revised model of atmospheric CO_2 over Phanerozoic time. *Am. J. Sci.* **294,** 56–91 (1994).
32. Grotzinger, J. P. & Kasting, J. F. New constraints on Precambrian ocean composition. *J. Geol.* **101,** 235–243 (1993).
33. Wadleigh, M. A. & Veizer, J. $^{18}O/^{16}O$ and $^{13}C/^{12}C$ in Lower Paleozoic articulate brachiopods: Implications for the isotopic composition of seawater. *Geochim. Cosmochim. Acta* **56,** 431–443 (1992).

Localization of the gravity field and the signature of glacial rebound

Mark Simons* & Bradford H. Hager

Department of Earth Atmospheric and Planetary Sciences, Massachusetts Institute of Technology, Cambridge, Massachusetts 02139, USA

The negative free-air gravity anomaly centred on Hudson Bay, Canada, shows a remarkable correlation with the location of the Laurentide ice sheet, suggesting that this gravity anomaly is the result of incomplete post-glacial rebound[1-3]. This region, however, is also underlain by higher-than-average mantle seismic velocities, suggesting that the gravity low might result instead from dynamic topography associated with convective downwellings[4-7]. Here we analyse the global gravity field as a simultaneous function of geographic location and spectral content. We find that the Hudson Bay gravity low is unique, with anomalously high amplitude in the spectral band where the power from the Laurentide ice load is greatest[2] and the relaxation times predicted for viable models of viscous relaxation are longest[8]. We estimate that about half of the Hudson Bay gravity anomaly is the result of incomplete post-glacial rebound, and derive a mantle viscosity model that explains both this gravity signature and the characteristic uplift rates for the central Laurentide and Fennoscandian regions[6]. This model has a jump in viscosity at 670 km depth, comparable to that in dynamic models of the geoid highs over subducted slabs[4,9], but lacks a low-viscosity asthenosphere, consistent with a higher viscosity in the upper mantle beneath shields than in oceanic regions.

Delayed rebound is not the dominant process generating variations in the global gravity field (Fig. 1a); many anomalies of comparable or greater amplitude than those in deglaciated areas

* Present address: Seismological Laboratory, California Institute of Technology, Pasadena, California 91125, USA.